

Local Corrosion Behavior of 2024 Alloy in NaCl Solution by EIS and SECM

He-Rong ZHOU^{a,*}, Shu-Peng SONG^b, Bi-Hua HU^c, Xin-Pei HONG^d

School of Materials and metallurgy, Wuhan University of Science and Technology, Wuhan, 430081, PR China

Email: azhouhr_9@163.com, bspsong@wust.edu.cn, c981150961@qq.com, d944959024@qq.com

Corresponding author: Zhou Herong

Keywords: Localized corrosion, 2024aluminum alloys, Intermetallic particles, SECM, EIS

Abstract: The corrosion behavior of 2024 alloy in 0.6 mol/L NaCl solution has been studied by EIS, SECM and SEM at the corrosion potential. The EIS results show that the pitting could have occurred between 2 hr and 6 hr immersion and the corrosion dissolution becomes severe with the increase of immersion time. The SECM results reveal that the redox value and the dissolution active sites on the sample surface change with the immersion time. The oxidation current value increases rapidly between 0-3 hrs immersion and keeps about the same quantitative level after long immersion (3-48hrs). SEM morphology indicates that the pitting on the surface of the specimen has happened. At last, a model of local dissolution on grain boundary is put forward and can maybe describe how the initial stage of the corrosion process happens. It could be beneficial to explain the dissolution of intermetallic precipitates or aluminum around the IMFS on the surface of the specimen result in high oxidation current value.

1. Introduction

In aluminum alloys, Si, Zn, Fe, Mn, Cu and Mg are introduced at various levels mainly to improve mechanical strength, e.g. 2024 alloy, which has been widely used in the aerospace industry due to its high strength-to-weight ratio, good fracture toughness and low cost. However, it is susceptible to corrosion and corrosion fatigue in the atmosphere [1].

There are some kinds of intermetallic precipitates (IMPs) in aluminum alloys. Their influence on pitting should be investigated in detail in order to understand the initial corrosion mechanism and control the corrosion of the material [2]. The pitting has a very significant effect on the use of aluminum alloy. Due to the complexity of the microstructure of multi-component aluminum alloys, the pitting mechanism for aluminum alloys is still not understood completely, especially regarding the influence of various kinds of intermetallic precipitates. Further studies are needed to know the role of intermetallic compounds and deterministic factors in the pitting initiation, e.g., second phase particle, the conditions of the pitting formation and so on [3]. The local measurement techniques (for instance, SECM, AFM and SKP) have also been shown capable to provide useful information [4~7]. SECM was also used to resolve the heterogeneous cathodic activity at AA2024 surfaces using Pt microelectrode and redox mediator. SECM images showed locally high redox reactivity that was attributed to intermetallic particles [8]. In some reports, SECM mapping was quite useful for corrosion behavior study and the initial dissolution behavior for materials. So, the use of SECM is helpful to study the mechanism of pitting corrosion. In addition, electrochemical impedance spectroscopy (EIS) can also be successfully used to analyze corrosion behavior in atmospheric corrosion researches [9–11].

This paper presents the results of the EIS test and SECM probing of 2024 alloy in 0.6 mol/L NaCl solutions. The corrosion morphology was observed by SEM, and it is explained by the corrosion theory of IMPs.

2. Experimental

2.1. Experimental Material

In the paper, a commercial 2024 alloy is used with its chemical composition (wt. %) Cu 4.68, Mg 1.58, Mn 0.53, Ti 0.023, Zn 0.10, Fe 0.35, Si 0.13, balanced by Al. The electrode was sealed by epoxy, leaving 1 cm² surfaces area exposed to the air to serve as a working electrode for electrochemical experiment. Before experiments, the exposed surface was polished down to 1.5 μ m diamond paste, then degreased in acetone and finally washed up by distilled water.

2.2. EIS Measurements

EIS tests were performed with PARSTAT 2273 electrochemical workstation. The electrolyte is 0.6 mol/L NaCl solution (pH 7.0) in contact with the air at about 20 \pm 4 $^{\circ}$ C. A traditional three electrodes system is used for EIS measurement. The working electrode is 2024 alloy with 1cm \times 1cm area exposed into the electrolyte, which Pt piece used as the counter electrode. A saturated calomel electrode is used as the reference electrode in this measurement. The employed amplitude of the sinusoidal signal for EIS tests is 5 mV, and the frequency span is 100 kHz –10 mHz. EIS tests are always conducted from high frequency to low frequency, and ZSimpWin 3.2 software is used for the data fitting of impedance spectra.

2.3. SECM Measurements

SECM experiments were carried out using scanning electrochemical microscopy 370 (SECM370) workstation of EG & G company. The instrument has a probe with three axes of transition (x, y, z). The Z axis is vertical to the plane formed by x axis and y axis. The plane is parallel to the aluminum alloy substrate electrode. The current value measured from SECM370 workstation is the current of redox reaction for I⁻ ion from the probe. Local high electrochemical current of the aluminum alloy surface will be detected due to the high redox oxidation current at a tip, as a result of increased redox reduction current at the dissolution sites on the aluminum alloy surface. The current value of oxidation reaction is used as a parameter to analyze the corrosion degree and the degree of local dissolution at E_{corr} [5].

The electrolyte is 0.6 mol/L NaCl solution (pH 7.0) in contact with the air at about 20 \pm 4 $^{\circ}$ C. 5mM KI which is chosen as the redox mediator for SECM mapping is joined to the electrolyte solution [5]. A traditional three electrode system used for this experiment is the same as those for EIS tests apart from a saturated Ag/AgCl as the reference electrode.

2.4. SEM Observation and EDX Analyses

The surface morphologies of the samples were observed using SEM and the compositional analysis of corrosion products was performed by energy dispersive X-ray detector (EDX) equipped with SEM.

3. Results and Discussion

3.1 Microstructural Characterization

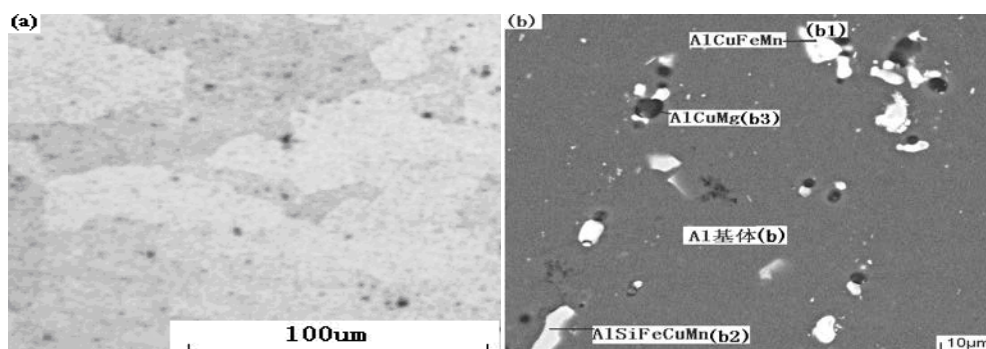


Fig.1. Microstructure of 2024 alloy: (a) micrograph; (b) SEM image.

Fig.1 shows microstructure morphology of 2A2 alloy (T4). 2024 alloy is composed of Al, Cu, Mg, Fe, Si and Mn elements and so on. There are some crystal boundaries and many intermetallic on the specimen surface from micrograph of 2024 alloy (Fig.1a). The intermetallic contain about Al₂Cu, Al₂CuMg, AlCuFeMn and AlCuFeMnSi (Fig.1b and Table.1) [12,13]. The intermetallic containing Cu, Si and Fe are cathodic with respect to the matrix in a corrosive solution and promote dissolution of the matrix because of different corrosion potential, while the intermetallic rich in Mg are anodic with respect to the matrix and dissolve preferentially [14].

Table.1 EDX analysis of intermetallic particles of 2024 alloy (wt %)

Dot	Si	Fe	Cu	Mn	Mg	Al
b	0.0	0.0	3.04	0.0	3.40	93.57
b1	0.0	11.01	32.77	2.48	0.0	53.57
b2	6.36	15.37	6.70	10.70	0.0	60.87
b3	0.0	0.0	6.58	0.0	2.47	90.25

3.2 Electrochemical Impedance Spectra

The EIS measurement in 0.6 M NaCl solution as a function of time is carried out at the corrosion potential (E_{corr}) (about -0.7 V vs saturated calomel electrode). The results in both Nyquist and phase formats are shown in Fig.2. There are two time constants visible in bode phase angle plots, especially at the time of 6h, 24h, 48h and 96h. But there is one time constant from bode phase angle plot of 2 hr (Fig.2b). In Niquist spectra, they all show one apparent capacitive semicircle and diffusion curve apart from Niquist curve for 2 hr immersion. These indicate that the corrosion behavior on the surface of the specimen has changed between 2hrs and 6hrs immersion, and the pitting could probably have occurred.

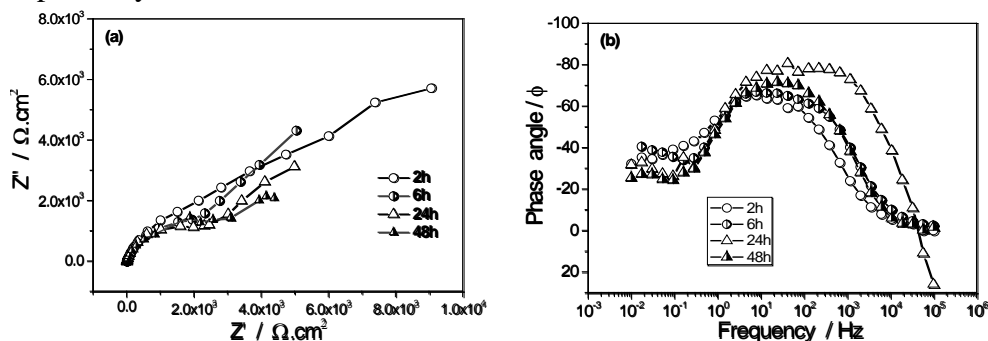


Fig.2. EIS plots for 2024 alloy in 0.6 mol/L NaCl solution (a)Nyquist and (b)phase angle plots

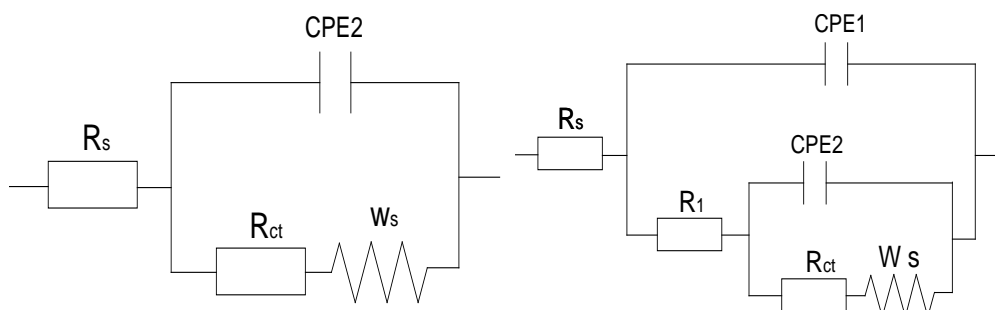


Fig.3 Equivalent circuit for the 2024 alloy in 0.6 mol/L NaCl solution: R_s is the solution resistance, (CPE)1 the outer layer capacitance including the passive film corrosion products, R_1 the resistance of the corrosion products and the pit pore, (CPE)2 the double layer capacitance of the anodic area and R_{ct} the charge transfer resistance

Fig.3 is an equivalent circuit, which is obtained through the structure of aluminum alloy electrode in Fig.6 and fitting EIS spectra in Fig.2. Equivalent circuit before 2 hrs immersion is shown in

Fig.3a, and Fig.3b after 6 hrs immersion. There are thin alumina film and corrosion products on the surface of the working electrode after long immersion. In an equivalent circuit, R_s is the solution resistance, $(CPE)_1$ shown as the outer layer capacitance including the passive film corrosion products, R_1 expressed to be the resistance of corrosion products and the pit pore, $(CPE)_2$ denoted as the double layer capacitance of the anodic area, w_s as diffusion resistance and R_{ct} indicated to be the charge transfer resistance of the double layer.

Based on the equivalent circuit, the typical EIS parameter can be worked out, which are listed in tables.2. In this paper, the reciprocal of the charge transfer resistance (R_{ct}) is used as a parameter to characterize the corrosion rate at E_{corr} . The value of R_{ct} decreases with the time prolonging from table. 2. The corrosion rate of 2024 alloy increases during 48 hrs immersion. The value of the double layer capacitance of the anodic area increases. These results show that the corrosion of 2024 alloy becomes severer with the increase of immersion time.

Table.2 The parameters of the EIS for 2024 alloy in 0.6 mol/L NaCl solution

Time	2h	6h	24h	48h
$R_s, \Omega \cdot \text{cm}^2$	13.6	5.2	6.1	4.2
$(Y_0)_1, \Omega^{-1} \text{cm}^{-2} \text{S}^{-n_1}$	1.33E-4	1.47E-4	1.21E-4	1.38E-4
n_1	0.79	0.79	0.85	0.85
$R_1, \Omega \cdot \text{cm}^2$		3.70E3	2.92 E3	3.48E3
$(Y_0)_2, \Omega^{-1} \text{cm}^{-2} \text{S}^{-n_2}$		9.78E-4	1.84E-3	2.42E-3
n_2		1.0	1.0	1.0
$R_{ct}, \Omega \cdot \text{cm}^2$	4.39E3	3.49E3	2.52E3	1.52E3
w_s	4.40 E-4	5.19 E-4	1.14E-3	1.50E-3

3.3 SECM topography

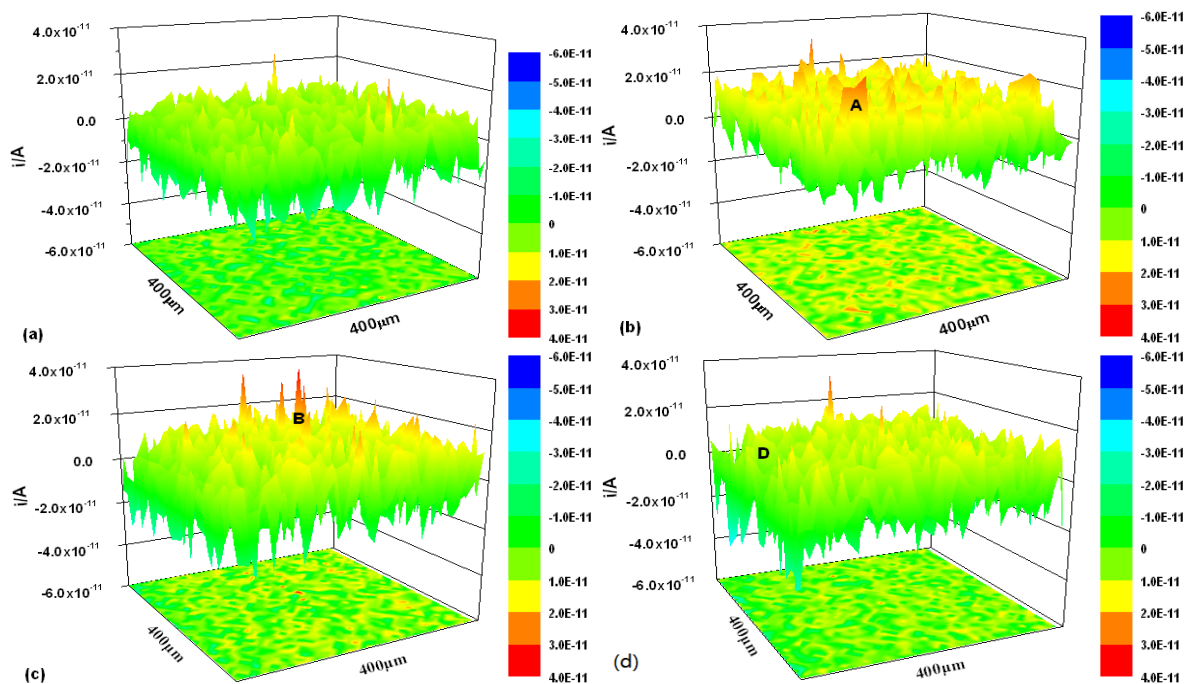


Fig.4. Current images obtained for 2024 alloy in 0.6 mol/L NaCl solution (scanning area $400\mu\text{m} \times 400\mu\text{m}$) (a)0.5h; (b)3h; (c)18h; (d) 48h

The corrosion behavior can be analyzed through observing SECM images of the samples immersed in the solution. Fig.4 shows in situ SECM observation of 2024 alloy in mol/L NaCl solution at corrosion potential (E_{corr}). The SECM morphologies (scanning area $400\mu\text{m} \times 400\mu\text{m}$) under the 3D

images show the variations in current and electrochemical activity. The high current value at some local sites explains how the active dissolution has happened. The active sites are the locations that the pitting is probably formed. Fig.4a reveals the surface current image when the specimen was immersed in the solution after 1 hour immersion. Distribution of oxidation current peak is symmetrical in testing region. The maximum current is about 2.4×10^{-11} A in two local areas. The current peak value on the probe means that this location is the site of active dissolution of intermetallic or aluminum. The detailed reason was expounded in paper [2, 5]. With increase of corrosion time, the current value over the same region becomes higher in Fig.4b, 4c and 4d. This suggests that the dissolution on the surface of 2024 alloy become intense. Fig.4b displays the surface current image after 3 hrs immersion. The current value is biggest in the A region. The current distribution image after 18 hrs immersion is indicated in Fig.4c, and the current value is maximal in the B region. Likewise, the current value after 40 hrs immersion is measured to be maximum in the C region. However, the lowest current value is shown in D region after 48 hrs immersion. These results mean that the sites of maximal current peak are varying with the increase of corrosion time. Namely, the site of the active dissolution is different in the same testing region.

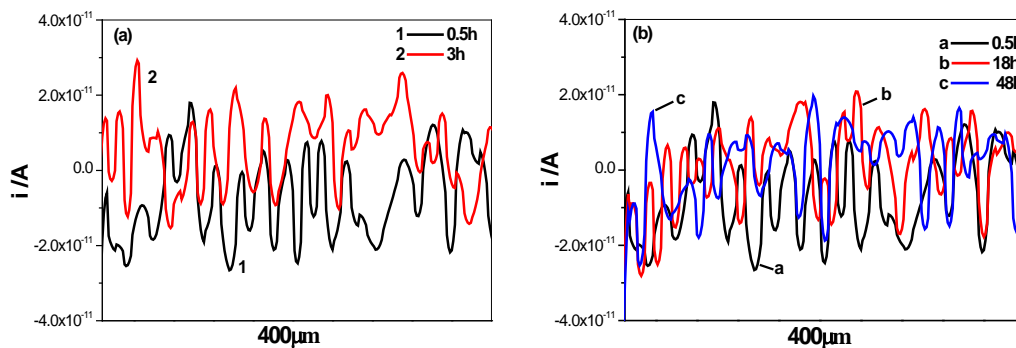


Fig.5 Line current images obtained for 2024 alloy in 0.6 mol/L NaCl solution (scanning curve from Fig.4) (a) initial stage of immersion, (b) the entire process of immersion

Line current images obtained for 2024 alloy in 0.6 mol/L NaCl solution are shown in Fig.5. The line profiles under the 2D images display current images of the same line region at E_{corr} . The oxidation current value is low at 1 hr immersion (curve 1 in Fig.5a). This means that local dissolution for 2024 alloy is very light and the active sites are few. Curve 2 in Fig.5a reveals that the surface current value tested after 3 hrs immersion increases rapidly and the peak number of the current value at local region becomes more. It indicates that the local active dissolution is very acute at 3 hr. The pitting on the surface of the specimen occurs at this moment. The difference of the current value between 18 hr and 48 hr immersion (from Fig.5b) is small, but the sites of local active dissolution vary. This means that the corrosion degree gradually increases.

3.4 SEM Morphology

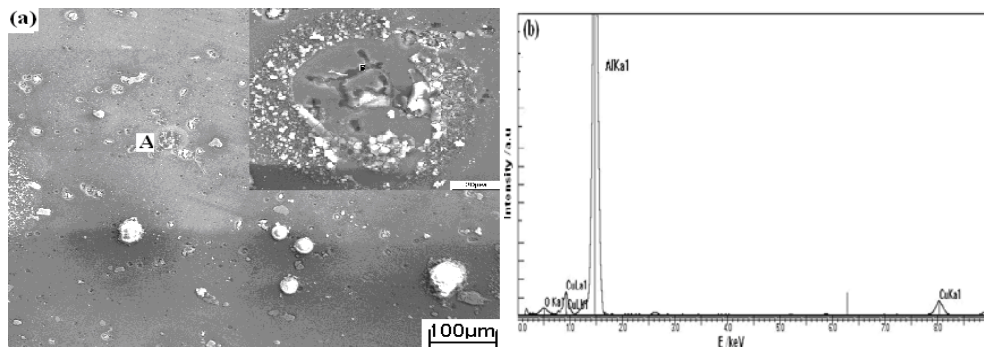


Fig.6. SEM morphologies and EDS result of 2024 alloy in 0.6 mol/L NaCl solution after 48h corrosion (a) SEM morphology; (b) EDS result.

SEM morphologies of 2024 alloy after 48 hrs immersion are shown in Fig.6. There are some small pits and many corrosion products on the surface (Fig.6a). This indicates that 2024 alloy has been eroded and the dissolution has occurred. From the zoom microstructure (from dot A in Fig.6a), localized dissolution mainly occurred on the grain boundary and around a particle. Element analysis for dot B within the round-shaped boundary is revealed in Fig.6b. There are Al, O and Cu elements, no Mg element from EDS results. It is explained that Mg element on the surface of the specimen has possibly been dissolved in 0.6 mol/L NaCl solution firstly.

3.5 Discussion

Davoodi A [2] had studied local dissolution of aluminum alloys in chloride solutions by AFM and SECM. He observed preferential dissolution in the boundary region between some intermetallic particles (IMPs) and alloy matrix, and trench formation around large IMPs during free immersion and under anodic polarization, which indicated different dissolution behavior associated with different types of IMPs. Moreover, simultaneous probing of electrochemical active sites and topographic changes over the same area was performed with submicron resolution. These results show ongoing localized dissolution related to intermetallic particles in the Al alloys, which may occur well below the breakdown potential.

After the sample for 2024 alloy was immersed in 0.6 mol/L NaCl solution, localized dissolution (namely localized corrosion) occurred in a particle, matrix or particle/matrix boundary region [2, 5]. During the ongoing corrosion process of aluminum alloys, different local dissolution behavior was observed by SEM and SECM (Fig.4 and Fig.6), which could mainly be attributed to different types of IMPs. The intermetallic for 2024 alloy contain Al₂Cu, Al₂CuMg, AlCuFeMn and AlCuFeMnSi and so on. The intermetallic rich in element Mg (e.g. Al₂CuMg et al) are anodic relative to the matrix Al, dissolved preferentially as the high potential, namely anodic dissolution (shown as Fig.7a)[14]. The intermetallic containing Cu and Fe (for instance Al₂Cu, AlCuFeMn, AlCuFeMnSi and so on) promote dissolution of the matrix because the potential for the intermetallic is lower than that for element Al, mainly Al dissolved preferentially (shown as Fig.7b). When the matrix Al around the intermetallic has been dissolved absolutely, the intermetallic will be exfoliated from the surface of the sample.

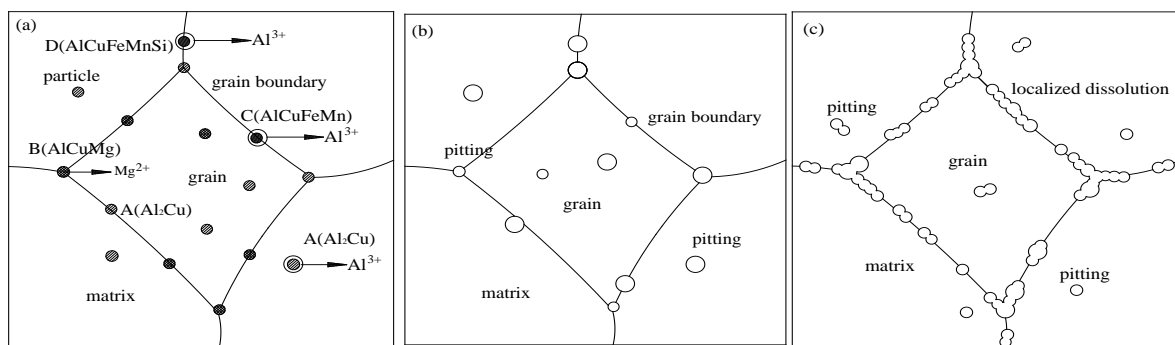


Fig.7. Local corrosion process of 2024 alloy immersed in 0.6 mol/L NaCl solution.

The localized dissolution for 2024 alloy means that the oxidation current tested from M370 workstation increases. The site of current peaks of oxidation reaction on the surface of the specimen is the location of localized dissolution for 2024 alloy [5]. With increase of immersion time, the current values of oxidation reaction over the same region become high (shown as Fig.4b, 4c, 4d and 4e). The current values after 3 hrs immersion are higher than that after 1 hr immersion (Fig.5a). It means that local dissolution becomes intense after 3 hrs immersions. The pit has possibly happened. But the current value after 18 hrs or 48 hrs immersions is lower than that after 3 hrs immersions, and keeping the same quantitative level (Fig.5b). And it implies that the dissolution degree of 2024 alloy become bigger and the corrosion is severe. The result is consistent with that from Fig.3.

The intermetallics or element Al for 2024 alloy on the grain boundary will probably be dissolved into 0.6 mol/L NaCl solution firstly because grain boundary possesses high energy. Black grain

boundary from the zoom morphology is formed in Fig.6a. This means that local corrosion for 2024 alloy has occurred and it is named as the pitting (e.g. dot A). The dissolution process at the initial stage of immersion is explained as Fig.7. Firstly, localized dissolution of intermetallic or element Al occurs on the grain boundary (Fig.7a). With increase of corrosion time, the small pit on the grain boundary started to come into being and the number of the pit increases (Fig.7b). Many pits on the grain boundary (Fig.7c) mean that the dissolution becomes severe and gradually the local corrosion namely the pit is formed finally.

4 Conclusion

EIS, SECM and SEM are used to investigate the corrosion behavior of 2024 alloy in 0.6 mol/L NaCl solution. The EIS analysis result shows that the pit occurs between 2hr and 6 hr immersion and the corrosion degree becomes severe with increase of immersion time. Local dissolution behavior on the grain boundary was observed by SECM and SEM, which the current value of oxidation reaction after different immersion time changes. The current value increases at the initial stage of immersion (about 3 hrs immersion) and keeps the same quantitative level at long immersion (between 18 hrs and 51 hrs immersion). Electrochemical dissolution of IMPs for 2024 alloy lead to the increase of the current value at some local regions. The SECM result is consistent with that of EIS analysis. The initial dissolution behavior for 2024 alloy could be explained. These results have contributed to search microscopic mechanism of pitting and further study for 2024 alloy.

5 Acknowledgements

The authors greatly acknowledge the supports of the National Natural Science Foundation of China (No. 50971048) and National material environmental corrosion platform. In addition, many thanks are due to Dr. Meng G Z for the assistance with the SECM measurements.

References

- [1] W.L. Zhang, G.S. Frankel, Transitions between pitting and intergranular corrosion in AA2024, *Electrochimica Acta*, 48(2003)1193-1210
- [2] A. Davoodi, J. Pana, C. Leygraf, Probing of local dissolution of Al-alloys in chloride solutions by AFM and SECM, *Applied Surface Science*, 252(2006) 5499-5503.
- [3] Z.S. Smialowska, Pitting corrosion of aluminum, *Corros. Sci.*, 41(1999)1743-1753.
- [4] J.H.W. de Wit, Local potential measurements with the SKPFM on aluminium alloys, *Electrochimica Acta*, 49(2004) 2841-2850
- [5] A. Davoodi, J Pana, C Leygraf, In situ investigation of localized corrosion of aluminum alloys in chloride solution using integrated EC-AFM/SECM techniques, *Electrochemical and Solid-State Letters*, 8(2005) B21-B24
- [6] Y.H. Shao, M.V. Mirkin. Probing ion transfer at the liquid/liquid interface by scanning electrochemical microscopy. *J. Phys. Chem.*, B102(1998) 9915-9921
- [7] C.H. Paik, H.S White, R.C. Alkire, Scanning electrochemical microscopy detection of dissolved sulfur species from inclusions in stainless steel, *J. Electrochem. Soc.*, 147(2000)4120-4127.
- [8] J.C Seegmiller, D.A Buttry, A SECM Study of heterogeneous redox activity at AA2024 surfaces, *J. Electrochem. Soc.*, 150(2003)B413-B419
- [9] A. Gamal EL-Mahdy, B Kwang. Kim, AC impedance study on the atmospheric corrosion of aluminum under periodic wet-dry conditions, *Electrochimica Acta*, 49(2004) 1937-1948

- [10] G.A El-Mahdy, A Nishikata, T Tsuru, AC impedance study on corrosion of 55%Al-Zn alloy-coated steel under thin electrolyte layers, *Corros. Sci.*42(2000) 1509-1521
- [11] M Stratmann, H Streckel, K.T Kim, S Crockett, On the atmospheric corrosion of metals which are covered with thin electrolyte layers-III. The measurement of polarization curves on metal surfaces which are covered by thin electrolyte layers, *Corros. Sci.* 30 (1990) 715-734.
- [12] R.G Buchheit, M.A Martinez, L.P Montes, Evidence for Cu ion formation by dissolution and dealloying the Al₂CuMg intermetallic compound in rotating ring-disk collection experiments, *J Electrochem.Soc.*, 147(2000)119-124.
- [13] R.G Buchheit, R.P Grant, P.F Hlavaa, Local dissolution phenomena associated with S phase (Al₂CuMg) particles in aluminum alloy 2024-T3, *J.Electrochem.Soc.*, 144 (1997)2621-2628
- [14] F Andreatta, M.M Lohrengel, H Terry, Electrochemical characterisation of aluminum AA7075-T6 and solution heat treated AA7075 using a micro-capillary cell, *Electrochimica Acta*,48(2003) 3239-3247